Multi-Material Topology Optimization with Continuous Magnetization Direction for motors design

Thomas Gauthey, P. Gangl, Maya Hage-Hassan

Multi-Material Topology Optimization with Continuous Magnetization Direction for motors design

T. Gauthey, P. Gangl and M. Hage Hassan

2022 International Conference on Electrical Machines (ICEM) | 978-1-6654-1432-6/22/$31.00 ©2022 IEEE | DOI: 10.1109/ICEM51905.2022.9910654

***Abstract*—Permanent magnet-assisted synchronous reluctance motors (PMSynRM) have a significantly higher average torque than synchronous reluctance motors. Thus, determining an optimal design results in a multi-material topology optimization problem, where one seeks to distribute ferromagnetic material, air and permanent magnets within the rotor in an optimal manner. In this paper, we propose the use of density-based distribution scheme, which allows for continuous magnetization direction. A filter using K-mean clustering is used to determine the magnetization angle final distribution accounting for technical feasibility. As for the ferromagnetic material interpolation, a novel interpolation scheme inspired by the topological derivative is established. A comparison with several interpolation schemes is proposed. Finally, the design of the electrical motor is proposed to maximize the torque value.**

***Index Terms*—Motors, Numerical models, Optimization, Permanent magnet machines**

I. Introduction

Synchronous reluctance machines (SynRM) are standard in households and industrial applications, thanks to their cheap cost compared to permanent magnet motors and advances in manufacturing techniques. Although the deployment of these machines continues [1], permanent magnet synchronous reluctance machines (PMSynRM) offer an excellent alternative for both structures, solving for SynRM, its poor power factor and, for permanent magnet machines (PMM), its cost. The design of these machines using parametric optimization often necessitates complex analytical models relying heavily on experienced engineers and known good designs [2].

Topology optimization based on Finite Element Analysis (FEA) allows for bypassing such cumbersome frameworks. Recently n-materials optimization of electromagnetic actuator has allowed for new PMM and SynRM to emerge [3]–[5]. In this paper, density based optimization is applied to design a PMSynRM. We propose a simultaneous density-based optimization scheme consisting of three materials (air/iron/magnet). The magnetization direction can be fixed or limited to a set of a couple values [6]–[9]. In this paper a continuous directions are considered during the optimization process as proposed in [10], [11]. Instead of fixing the mean value of the magnetization direction, the final directions are filtered using an unbiased K-means heuristic.
In density based topology optimization, the quality of the final solution is dependent on the choice of interpolation functions. We propose a novel interpolation based on properties of the topological derivative. It also takes into account the Marrocco BH-curve parameters. The proposition is applied to design the rotor of a distributed winding stator as described in [12], [13] to maximize the mean torque under constraints. Finally, to decrease computation time, torque for the PMSynRM is computed through a four-point method.

T. Gauthey is with the Group of electrical engineering, Paris, 91192, Gif-sur-Yvette, France (e-mail: thomas.gauthey@centralesupelec.fr).
P. Gangl is with Technische Universität Graz, Institut für Angewandte Mathematik, 8010 Graz, Austria (e-mail: gangl@math.tugraz.at)
M. Hage Hassan is with the Group of electrical engineering, Paris, 91192, Gif-sur-Yvette, France (e-mail: maya.hage-hassan@centralesupelec.fr)

II. Problem description

We chose to investigate a SynRM described in [12], [13], of which the rotor design had proven to be a challenging problem for topology optimization and use it for our PM-SynRM optimization problem.

A. Geometry description

The electrical machine geometry and current density distributions are given respectively in Figure 1 and 2. The dimensions for the considered machine are given in Table I.

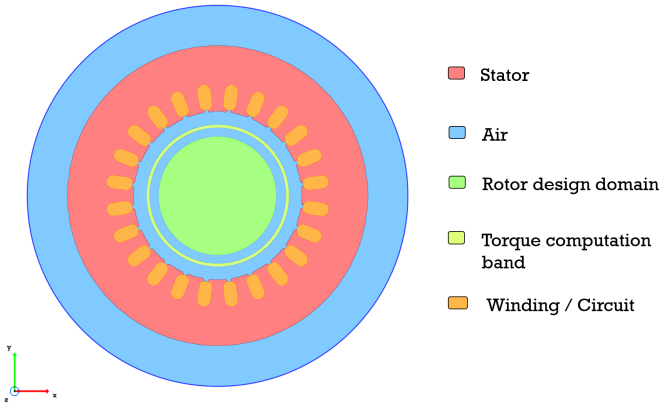

Fig. 1. Machine geometry

This machine differs from most conventional SynRM by its large air gap which constrains the statoric winding distribution to only one pair of poles (cf. Figure 2).

TABLE I
GEOMETRIC PARAMETERS

Parameter	Value
Slot number	24
Axial length	50.0 mm
Outer rotor radius	18.5 mm
Inner stator radius	26.5 mm
Outer stator radius	47.5 mm
Air gap length	8.0 mm

TABLE II
STATORIC WINDING PARAMETERS

Parameter	Value
Number of turn N_s	64
Winding type	Distributed
Connection type	Star
Resistance ($R_{S,20°C}$)	7.1 Ω
Voltage U_{eff}	230 V
Peak intensity I_{max}	12 A
Number of pole pairs n_{pp}	1

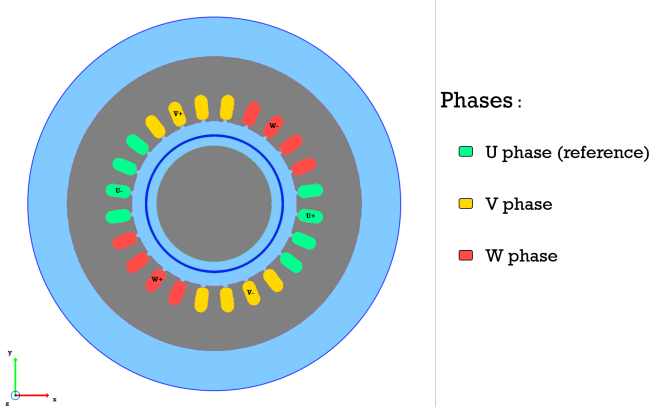

Fig. 2. Statoric winding distribution and current parameters

The computational domain Ω consists of iron Ω_f , air Ω_{air}, permanent magnet Ω_{mag} and coils Ω_c,

$$\Omega = \Omega_f \cup \Omega_{air} \cup \Omega_{mag} \cup \Omega_c \tag{1}$$

where we further subdivide the ferromagnetic and air subdomains into their rotor $\Omega_{f,rot}$ and stator parts $\Omega_{f,stat}$,

$$\Omega_f = \Omega_{f,stat} \cup \Omega_{f,rot}, \qquad \Omega_{air} = \Omega_{air,stat} \cup \Omega_{air,rot}. \tag{2}$$

Moreover, we subdivide the coil subdomains according to the distribution shown in Figure 2,

$$\Omega_c = \Omega_{U^+} \cup \Omega_{U^-} \cup \Omega_{V^+} \cup \Omega_{V^-} \cup \Omega_{W^+} \cup \Omega_{W^-}. \tag{3}$$

We present here after the properties of interest of the materials (air, ferromagnetic, magnet) used in the machine.

The maximum norm of the magnetization vector was chosen as $M_{max} = 2.33 \cdot 10^5 A.m^{-2}$ to fit data from [14] on ferrite magnets. The reluctivity of the magnets and of the copper coils is assimilated to the one of air to simplify further material interpolation and avoid complex schemes like the ones found in [15]. The non-linear behaviour of the ferromagnetic material is modelled with a Marrocco's BH curve approximation [16],

TABLE III
MATERIAL PROPERTIES

Material	Reluctivity $[m.H^{-1}]$	Magnetization $[A.m^{-1}]$
Air	ν_0	0
Copper	ν_0	0
Ferromagnetic	$\hat{\nu}(\lvert\vec{B}\rvert)$	0
Magnet	ν_0	M_{max}

$$\hat{\nu}(|\vec{B}|) = \begin{cases} \nu_0(\varepsilon + \frac{(c-\varepsilon)|\vec{B}|^{2\alpha}}{\tau+|\vec{B}|^{2\alpha}}, & \text{if } |\vec{B}| \leq B_{max}, \\ \nu_0 \left(1 - \frac{M_s}{|\vec{B}|}\right) & \text{else if } |\vec{B}| > B_s, \\ exp\left(\frac{\gamma(|\vec{B}|-\beta)}{|\vec{B}|}\right) & \text{otherwise,} \end{cases} \tag{4}$$

where $B_s = \beta + \frac{log(\frac{\nu_0}{\gamma})}{\gamma}$ and $M_s = B_s + \frac{1}{\gamma}$ and the coefficients of the Marrocco curve are defined in Table IV.

TABLE IV
MARROCCO CURVE COEFFICIENT FOR THE FERROMAGNETIC MATERIAL

Parameter	Value
α	6.84
β	-1.30·10^{-1}
γ	4.86
ε	1.57 ·10^{-4}
τ	4.14 ·10^3
c	1.90·10^{-2}
B_{max}	1.80 (T)

B. Torque computation method

For computing the torque, we chose a method based on Maxwell's stress tensor, Arkkio's method [17]. The instantaneous is given such that :

$$T = \frac{L_z \nu_0}{r_s - r_r} \int_S \sqrt{x^2 + y^2} B_r B_\phi dS \tag{5}$$

where B_r and B_ϕ denote the radial and tangential magnetic induction, respectively, L_z denotes the length of the machine in z-direction and S denotes the surface between radii r_s and r_r in the air gap (with $r_s > r_r$).

Determining the average torque by means of its instantaneous values can be very expensive. It is shown in [18] that a good torque approximation for PMSM can be obtained when evaluating its value for suitably chosen rotor positions θ:

$$\bar{T} = \frac{1}{4}\left(T_0 + T_{\frac{\pi}{12}} + T_{\frac{\pi}{6}} + T_{\frac{\pi}{4}}\right). \tag{6}$$

We compared the average torque obtained by evaluation at 500 equally distributed rotor positions between 0 and 2π with the value obtained by the four-point formula (6). When the torque value is not equal to zero, the error found was to be lower than 1% as expected and described in literature [19]. For the design given in Fig. 14, torque calculated on 500 points is equal to 1.9 [N.m] and through $4point$ 1.88 [N.m] with an error of 0.5%

III. Optimization problem

In this section, we define our optimization problem and reformulate the forward problem to fit the density-based topology optimization approach. Our goal is to maximize the average torque computed via (6) by distributing iron and permanent magnets. The iron is represented by the variable ρ_ν, and the permanent magnets by two variables ρ_{M_x} and ρ_{M_y} to take into account the magnets direction.

$$(P_1): \begin{cases} \text{maximize } \bar{T} \\ \text{Under constraints :} \\ \text{Volume}(\rho_\nu) \leq f_{v,iron} \\ \text{Volume}(\rho_{M_x}, \rho_{M_y}) \leq f_{v,mag} \end{cases} \tag{7}$$

$f_{v,iron}$, $f_{v,mag}$ are respectively the volume fractions of iron and magnet. Lancelot method a gradient based optimization algorithm [20] is used to solve the reformulated problem, considering the augmented Lagrangian merit function.
The gradient of the Lagrangian is determined by means of adjoint method [21], [22]. The objective function is determined by solving the magnetostatics problem (8) on NGSolve.

$$\begin{aligned} \text{Find } u \in H_0^1(\Omega) : \int_\Omega \nu(x, |\nabla u|)\nabla u \cdot \nabla v \, dx = \\ \int_{\Omega_c} j\, v \, dx + \int_{\Omega_{mag}} \begin{bmatrix} -M_y \\ M_x \end{bmatrix} \cdot \nabla v \, dx, \quad \forall v \end{aligned} \tag{8}$$

A. Density based topology optimization

The basis of topology optimization is to distribute matter. In order, to solve it by means of gradient based algorithms, variables must be defined as continuous. Thus, the three density variables defined earlier, $\rho_\nu, \rho_{M_x}, \rho_{M_y}$ are interpolated by means of f_ν and f_M. The equation (8), is then rewritten such that :

$$\begin{aligned} &\int_\Omega \nu(\rho_\nu, |\nabla u|)\nabla u \cdot \nabla v \\ &- \int_{\Omega_{rot}} f_\nu(1-\rho_\nu) \frac{M_{max} f_M(|\vec{M}|)}{|\vec{M}|} \begin{bmatrix} -M_y \\ M_x \end{bmatrix} \cdot \nabla v \\ &= \int_{\Omega_c} j\, v \, dx, \end{aligned} \tag{9}$$

with the reluctivity function

$$\nu(\rho_\nu, |\nabla u|) = \begin{cases} \hat{\nu}(|\nabla u|) & \text{in } \Omega_{f,stat} \\ \nu_0 & \text{in } \Omega_c \cup \Omega_{air,stat} \\ \nu_0 + f_\nu(\rho_\nu)(\hat{\nu}(|\nabla u|) - \nu_0) & \text{in } \Omega_{rot} \end{cases} \tag{10}$$

Here, the components of the magnetization vector $\vec{M} = (M_x, M_y)$ are given in dependence of the two rotated density variables ρ_{M_x}, ρ_{M_y}, for a mapping $\tilde{f}_{sd}$,

$$(M_x, M_y) = \tilde{f}_{sd}(\rho_{M_x}, \rho_{M_y}), \tag{11}$$

which will be defined in (17).

B. Material interpolation schemes

In density based topology optimization, the quality of the final solution is dependant on the choice of interpolation functions. We present here two existing schemes and a novel one based on properties of the topological derivative.
The polynomial interpolation scheme :

$$f_n(\rho) = \rho^n \quad n > 0, \tag{12}$$

also referred to as SIMP (Solid Isotropic Material with Penalization), is the most used material interpolation scheme for topology optimization and allows for easy penalization of intermediate materials. However, it presents some symmetry issues and favors low ρ associated material in the final design. In [23], the authors compared this scheme to other schemes and concluded that the final design was not as good as many other proposed ones.

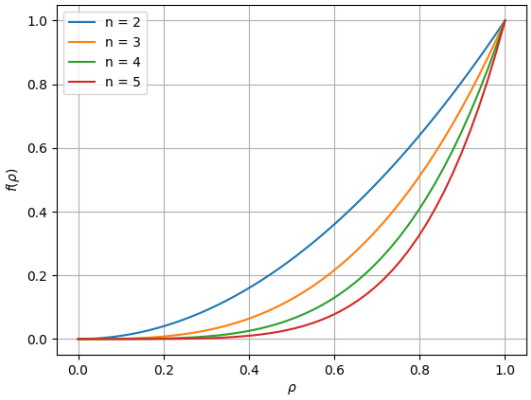

Fig. 3. SIMP Polynomial interpolation scheme

To solve symmetry issues introduced by the classical polynomial interpolation, D. Lukàš introduced a new scheme in [24]:

$$f_\lambda(\rho) = \frac{1}{2}\left(1 + \frac{1}{\arctan(\lambda)} \arctan(\lambda(2\rho - 1))\right), \quad \lambda > 0. \tag{13}$$

In this equation the particular invariant point $\rho = 0.5$ does not promote intermediate materials, grey material depends on λ values (cf. Figure 4).

High λ values permit to penalize intermediate materials but can lead to a poor convergence of the algorithm. A parameter study for λ led us to choose $\lambda = 5$. This interpolation method is chosen for the norm of the magnetization vector (f_M in (9)). Finally, we propose a new interpolation scheme as given in Figure 5, which is inspired by the topological derivative as done in [25], see also the the SIMP-All method for linear elasticity [26]. Here, we seek to design a material interpolation function whose derivative with respect to the density variable ρ coincides with the topological derivative of the problem at $\rho = 0$ and $\rho = 1$. When interpolating

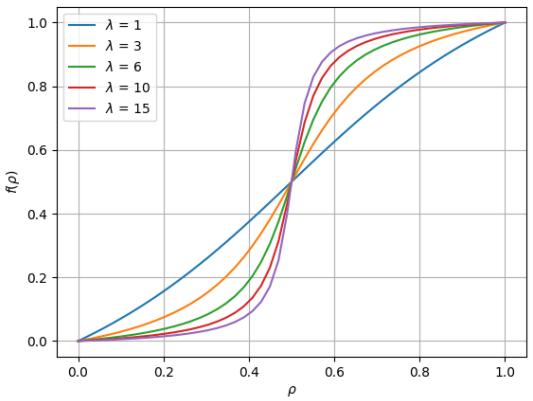

Fig. 4. D. Lukàš's interpolation scheme

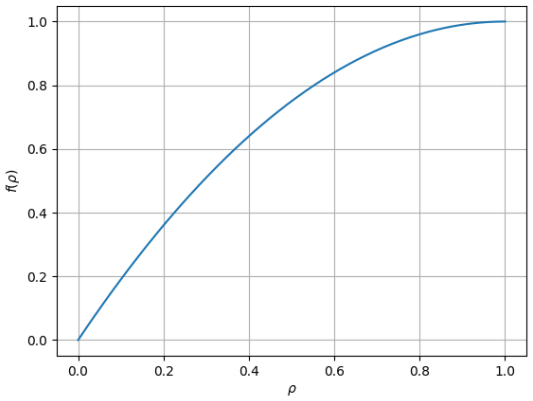

Fig. 5. Topological derivative inspired interpolation scheme

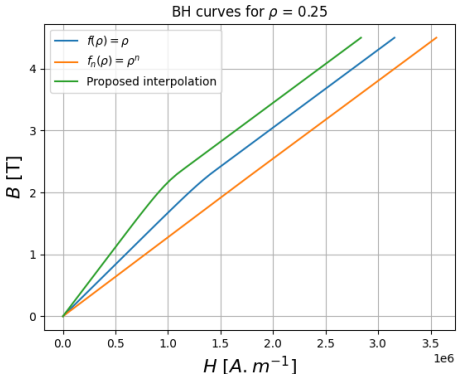

Fig. 6. Interpolated BH curve for $\rho = 0.25$

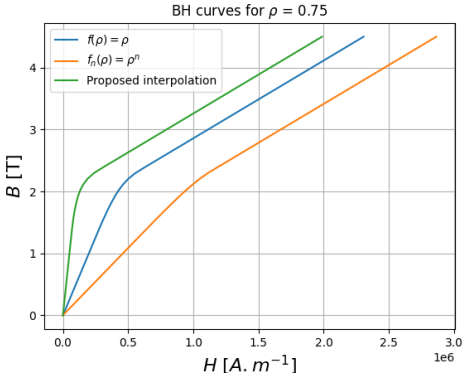

Fig. 7. Interpolated BH curve for $\rho = 0.75$

between two linear materials with reluctivity values ν_0 and ν_1, the conditions for the material interpolation function f according to [25] would read

$$\begin{cases} f(0) = 0, \\ f(1) = 1, \\ f'(0) = \frac{2\nu_0}{\nu_0+\nu_1}, \\ f'(1) = \frac{2\nu_1}{\nu_0+\nu_1}. \end{cases} \tag{14}$$

Due to the involved formula of the topological derivative for nonlinear magnetostatics [27], a mathematically rigorous extension of this method to the nonlinear setting is not straightforward. However, inspired by the particular behaviour of the Marrocco BH-curve where the magnetic reluctivity is almost constant for low flux density values, we simply use this idea for that constant reluctivity value $\nu_1 := \nu_0\varepsilon \approx 124.94$. Using cubic Hermite interpolation for the conditions (14), we obtain the polynomial

$$f(\rho) = \frac{2\nu_0}{\nu_0+\nu_1}\rho - \frac{\nu_0-\nu_1}{\nu_0+\nu_1}\rho^2. \tag{15}$$

Note that the term of order 3 happens to vanish. This interpolation is not equivalent to a penalization of $n = -1$ in (12), that may lead to convergence issues. The behaviour of the BH curve is compared for two ρ values of 0.25 and 0.75, when $n = 1$, $n = 3$ and the proposed method in Figures 6 and 7 .

We deal with two magnetization density variables $\rho_{M_x}, \rho_{M_y} : \Omega \to [0, 1]$ in order to represent the magnetization direction (M_x, M_y). One way of relating these quantities to each other would be to have ρ_{M_x} represent the first and ρ_{M_y} the second coordinate, resulting in a representation in Cartesian coordinates, which was also considered in [10]. In this case, however, some magnetization directions exhibit higher maximum magnetization than others, e.g. $\rho_{M_x} = \rho_{M_y} = 1$ would correspond to $|(M_x, M_y)^\top| = \sqrt{2}$ whereas for the magnetization direction pointing to the right $\rho_{M_x} = 1$, $\rho_{M_y} = 0.5$ would yield a maximum magnetization of $|(M_x, M_y)^\top| = 1$, thus making the maximum magnetization angle dependent.

To maintain the Cartesian coordinates, several mapping methods permit to realize a square-to-disk transformation, avoiding an angle dependent maximum magnetization value. The elliptic grid mapping was chosen as a good compromise

regarding computational time [28].

$$f_{sd}(x,y) = \begin{cases} x\sqrt{1-\frac{y^2}{2}} \\ y\sqrt{1-\frac{x^2}{2}} \end{cases} \quad \text{with } (x,y) \in [-1,1]^2. \quad (16)$$

The mapping between the magnetization density variables ρ_{M_x}, ρ_{M_y} and the magnetization vector $\vec{M} = (M_x, M_y)$ (11) is then given by

$$\tilde{f}_{sd}(\rho_{M_x}, \rho_{M_y}) = f_{sd}(2(\rho_{M_x} - 0.5), 2(\rho_{M_y} - 0.5)) \quad (17)$$

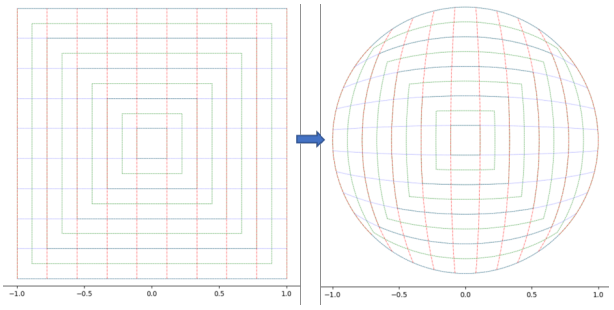

Fig. 8. Square to disk transform for the Magnetization vector coordinates

C. Filtering and Post-processing

In density-based topology optimization, checkerboard patterns and small isolated elements of one material are avoided using filtering methods at each step of gradient descent. While this filtering has a regularizing effect on the density variables, it may introduce more gray areas. In our approach, in the first step we perform density filtering using Helmholtz filter [29]. Some final designs can still present fuzzy boundaries and intermediate material, especially if the optimization starting point is near a local minimum. To help overcome this issue, we propose to penalize the intermediate materials directly as done in the phase-field topology optimization method [30] and add to the cost function the following term with a weight $\gamma > 0$:

$$I_\gamma(\rho) = \frac{4\gamma}{V_{\Omega_{rot}}} \int_{\Omega_{rot}} \rho(x)(1-\rho(x))dx. \quad (18)$$

The penalization is only applied on iron density ρ_ν and the magnetization norm $|\vec{M}|$. In our optimization problem we look for permanent magnetization directions which may change continuously in space. In order to obtain designs which comply with feasibility constraints, we here propose a post-processing step. A K-mean heuristic [31] clustering method is applied. We suggest adapting it to create clusters of elements of similar magnetization direction.

IV. Application to Design the Motor

All computations were conducted using the NGSolve [32], [33] framework with its python interface. SIMP method is based on gradient algorithm, thus the result depends on the starting point. Here, Two starting points are presented. The first starting point considers homogeneous material density in the design domain $\Omega_{f,rot}$. ρ_ν is fixed at 0.5, as given in Fig.9. As expected, magnets given in blue are distributed on the air barriers domain Fig.10. In topology optimization, traditionally this kind of method is initialized with an unbiased homogeneous distribution, but when considering synchro-reluctant machine design, flux barriers improve torque density. In [34] authors found low iron losses when considering five segments. Thus we proposed to initialize our geometry with the density distribution given in Fig. 11.

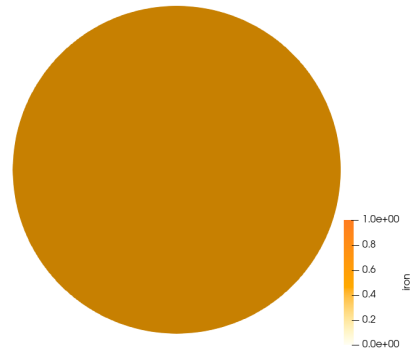

Fig. 9. Homogeneous starting point , $\rho_\nu = 0.5$

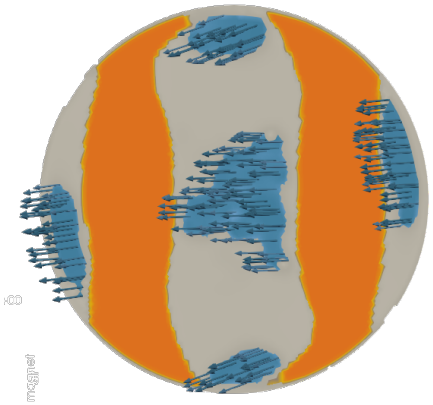

Fig. 10. Multimaterial, $f_{v,iron} = 40\%$, $f_{v,mag} = 30\%$, $\bar{T} = 1.42$N.m

The results for the material distribution are given for 20% and 40% of volume fractions $f_{v,iron}$. These results are coherent with the literature of synchro-reluctant actuators with distributed winding [34]. For the multi-material topology optimization including magnets, the design obtained at 40% (Fig.13) of ferromagnetic material is used as a starting point. Magnets are distributed in flux barriers as the first result Fig.10. We have a better torque that is probably due to high magnets volume, but this optimal result takes into consideration design requirements of synchro-reluctant motors.

V. Conclusion and Outlooks

In this study we proposed a novel multi-material interpolation method to determine the optimal distribution of

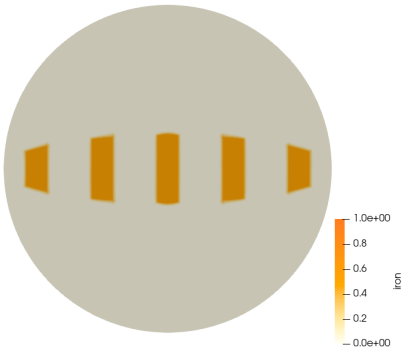

Fig. 11. Starting design

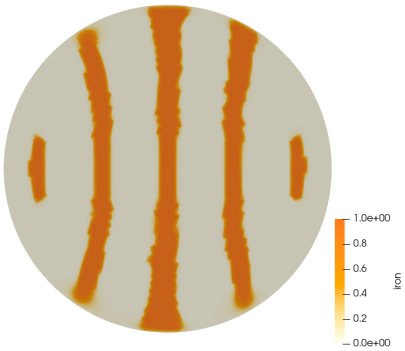

Fig. 12. Design Iron-Air, $f_{v,iron} = 20\%$, $\bar{T} = 0.833$N.m

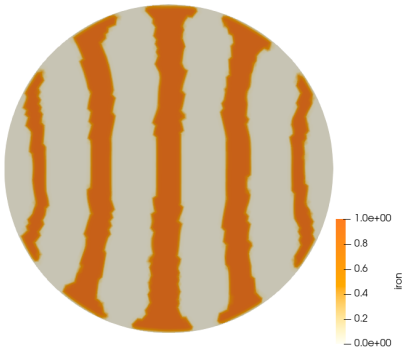

Fig. 13. Design Iron-Air, $f_{v,iron} = 40\%$, $\bar{T} = 1.12$N.m

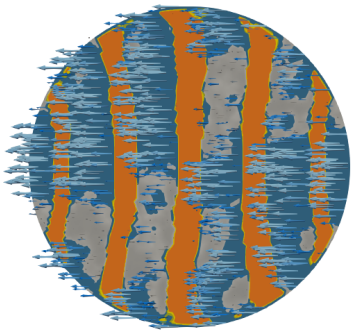

Fig. 14. Multimaterial, $f_{v,iron} = 40\%$, $f_{v,mag} = 50\%$, $\bar{T} = 1.85$N.m

air, iron, and magnets for PMSynRM. A novel interpolation method is proposed to take into consideration the material's BH curve. The interpolation takes into account magnetization amplitudes and direction, and a post-processing clustering method is also suggested to homogenize magnets direction for feasibility constraints.

REFERENCES

[1] H. Heidari, A. Rassõlkin, A. Kallaste, T. Vaimann, E. Andriushchenko, A. Belahcen, and D. V. Lukichev, "A Review of Synchronous Reluctance Motor-Drive Advancements," *Sustainability*, vol. 13, no. 2, p. 729, 1 2021.

[2] S. S. Maroufian and P. Pillay, "PM assisted synchronous reluctance machine design using AlNiCo magnets," in *2017 IEEE International Electric Machines and Drives Conference (IEMDC)*. Miami, FL, USA: IEEE, 5 2017, pp. 1–6.

[3] J. Kim, K. H. Sun, W. Kim, and J. E. Kim, "Magnetic torque maximization in a camera shutter module by the topology optimization," *J Mech Sci Technol*, vol. 24, no. 12, pp. 2511–2517, 12 2010.

[4] F. Guo, M. Salameh, M. Krishnamurthy, and I. P. Brown, "Multi-material Magneto-Structural Topology Optimization of Wound Field Synchronous Machine Rotors," *IEEE Transactions on Industry Applications*, vol. 56, no. 4, pp. 3656–3667, 2020.

[5] H. Sato, S. Hiruma, and H. Igarashi, "Multi-material topology optimization of permanent magnet motor with arbitrary adjacency relationship of materials," in *2020 IEEE 19th Biennial Conference on Electromagnetic Field Computation (CEFC)*, 2020, pp. 1–4.

[6] M. Risticevic, D. Iles, and A. Moeckel, "Design of an interior permanent magnet synchronous motor supported by the topology optimization algorithm," in *2016 International Symposium on Power Electronics, Electrical Drives, Automation and Motion (SPEEDAM)*. Capri, Italy: IEEE, 6 2016, pp. 221–225.

[7] J. Lee, E. M. Dede, and T. Nomura, "Simultaneous Design Optimization of Permanent Magnet, Coils, and Ferromagnetic Material in Actuators," *IEEE Transactions on Magnetics*, vol. 47, no. 12, pp. 4712–4716, 2011.

[8] J. S. Choi and J. Yoo, "Optimal design method for magnetization directions of a permanent magnet array," *Journal of Magnetism and Magnetic Materials*, vol. 322, no. 15, pp. 2145–2151, 2010.

[9] J. S. Choi, J. Yoo, S. Nishiwaki, and K. Izui, "Optimization of Magnetization Directions in a 3-D Magnetic Structure," *IEEE Transactions on Magnetics*, vol. 46, no. 6, pp. 1603–1606, 2010.

[10] S. Wang, D. Youn, H. Moon, and J. Kang, "Topology optimization of electromagnetic systems considering magnetization direction," *Magnetics, IEEE Transactions on*, vol. 41, pp. 1808 – 1811, 2005.

[11] T. Ishikawa, P. Xie, and N. Kurita, "Topology Optimization of Rotor Structure in Permanent Magnet Synchronous Motors Considering Ease of Manufacturing," *IEEJ Journal IA*, vol. 4, no. 4, pp. 469–475, 2015.

[12] C. Mellak, K. Krischan, and A. Muetze, "Synchronous Reluctance Machines as Drives for Rotary Anode X-Ray Tubes-A Feasibility Study," in *2018 XIII International Conference on Electrical Machines (ICEM)*. Alexandroupoli: IEEE, 9 2018, pp. 2613–2618.

[13] P. Gangl, S. Köthe, C. Mellak, A. Cesarano, and A. Mütze, "Multi-objective free-form shape optimization of a synchronous reluctance machine," *arXiv:2010.10117 [cs, math]*, 10 2020, arXiv: 2010.10117.

[14] A. S. Nunes, L. Daniel, M. Hage-Hassan, and M. Domenjoud, "Modeling of the magnetic behavior of permanent magnets including ageing effects," *Journal of Magnetism and Magnetic Materials*, vol. 512, p. 166930, 10 2020.

[15] W. Zuo and K. Saitou, "Multi-material topology optimization using ordered SIMP interpolation," *Struct Multidisc Optim*, vol. 55, no. 2, pp. 477–491, 2 2017.

[16] A. Marrocco, "Analyse numérique de problèmes d'électrotechnique," *Ann. Sc. Math. Québec*, vol. 1, no. 2, pp. 271–296, 1977.

[17] N. Sadowski, Y. Lefevre, M. Lajoie-Mazenc, and J. Cros, "Finite element torque calculation in electrical machines while considering

the movement," *IEEE Trans. Magn.*, vol. 28, no. 2, pp. 1410–1413, 3 1992.
[18] N. Bianchi, L. Alberti, M. Popescu, and T. Miller, "MMF Harmonics Effect on the Embedded FE-Analytical Computation of PM Motors," in *Conference Record - IAS Annual Meeting (IEEE Industry Applications Society)*, 2007, pp. 1544 – 1551.
[19] P. Akiki, M. Hage-Hassan, M. Bensetti, J.-C. Vannier, D. Prieto, and M. McClelland, "Axial ferrite-magnet-assisted synchronous reluctance motor," in *2018 XIII International Conference on Electrical Machines (ICEM)*, 2018, pp. 583–589.
[20] J. Nocedal and S. J. Wright, Eds., *Penalty, Barrier, and Augmented Lagrangian Methods*. New York, NY: Springer New York, 1999, pp. 488–525.
[21] G. Allaire, "A review of adjoint methods for sensitivity analysis, uncertainty quantification and optimization in numerical codes," *Ingénieurs de l'Automobile*, vol. 836, pp. 33–36, Jul. 2015. [Online]. Available: https://hal.archives-ouvertes.fr/hal-01242950
[22] R. El Bechari, F. Guyomarch, and S. Brisset, "The adjoint variable method for computational electromagnetics," *Mathematics*, vol. 10, no. 6, 2022. [Online]. Available: https://www.mdpi.com/2227-7390/10/6/885
[23] S. Sanogo and F. Messine, "Topology optimization in electromagnetism using SIMP method: Issues of material interpolation schemes," *COMPEL*, vol. 37, no. 6, pp. 2138–2157, 11 2018.
[24] D. Lukáš, "An Integration of Optimal Topology and Shape Design for Magnetostatics," in *Scientific Computing in Electrical Engineering*, A. M. Anile, G. Alì, and G. Mascali, Eds. Berlin, Heidelberg: Springer Berlin Heidelberg, 2006, pp. 227–232.
[25] S. Amstutz, C. Dapogny, and À. Ferrer, "A consistent relaxation of optimal design problems for coupling shape and topological derivatives," *Numerische Mathematik*, vol. 140, no. 1, pp. 35–94, 3 2018.
[26] A. Ferrer, "Simp-all: A generalized simp method based on the topological derivative concept," *International Journal for Numerical Methods in Engineering*, vol. 120, no. 3, pp. 361–381, 2019.
[27] S. Amstutz and P. Gangl, "Topological derivative for the nonlinear magnetostatic problem," *Electron. Trans. Numer. Anal.*, vol. 51, pp. 169–218, 2019.
[28] C. Fong, "Analytical methods for squaring the disc," 2019.
[29] B. S. Lazarov and O. Sigmund, "Filters in topology optimization based on Helmholtz-type differential equations," *Int. J. Numer. Meth. Engng.*, vol. 86, no. 6, pp. 765–781, 5 2011.
[30] H. Garcke, C. Hecht, M. Hinze, and C. Kahle, "Numerical Approximation of Phase Field Based Shape and Topology Optimization for Fluids," *SIAM J. Sci. Comput.*, vol. 37, no. 4, pp. A1846–A1871, 1 2015.
[31] J. MacQueen and others, "Some methods for classification and analysis of multivariate observations," in *Proceedings of the fifth Berkeley symposium on mathematical statistics and probability*, vol. 1. Oakland, CA, USA, 1967, pp. 281–297, issue: 14.
[32] P. Gangl, K. Sturm, M. Neunteufel, and J. Schöberl, "Fully and Semi-Automated Shape Differentiation in NGSolve," *arXiv:2004.06783 [math]*, 10 2020, arXiv: 2004.06783.
[33] J. Schöberl, "C++11 Implementation of Finite Elements in NGSolve," Institute for Analysis and Scientific Computing, Tech. Rep., 9 2014.
[34] A. Vagati, G. Franceschini, I. Marongiu, and G. Troglia, "Design criteria of high performance synchronous reluctance motors," in *Conference Record of the 1992 IEEE Industry Applications Society Annual Meeting*, 1992, pp. 66–73 vol.1.

VI. Biographies

Thomas Gauthey is currently a Masters student at CentraleSupelec Université Paris-Saclay. He is also with the Group of electrical engineering, Paris (GeePs). He did his internship at Graz University of Technology, his research interests include topology optimization and its applications to electrical engineering.

Peter Gangl received his BSc (2010), MSc (2012) and PhD (2017) in Applied Mathematics from Johannes Kepler University Linz, Austria. During his studies, he spent some time in Lund (Sweden), Berlin (Germany) and Avignon (France). Currently, he is a post-doctoral researcher at the Friedrich-Alexander University of Erlangen-Nürnberg, Germany, where he is on leave from his position as a university assistant at Graz University of Technology, Austria. His research interests include shape and topology optimization from both a theoretical and an application point of view, in particular for applications from electrical engineering.

Maya Hage-Hassan received her B.S. degree in mechanical engineering from the Faculty of engineering, Lebanon, Masters in Product Design and Development from Ecole Centrale de Nantes in 2010 and a Ph.D. degree in electrical engineering from University Paris-Saclay in 2014. She is currently Associate Professor in the Energy Department at CentraleSupelec. She is also with the Group of electrical engineering, Paris (GeePs). Her research interests include multiphysics design and optimization of electric machines and drives.